Available on CMS information server

**CMS DP -2024/065**

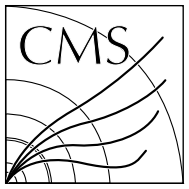

**The Compact Muon Solenoid Experiment**

CMS Performance Note

Mailing address: CMS CERN, CH-1211 GENEVA 23, Switzerland

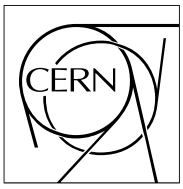

**16 July 2024**

# Muon momentum calibration with proton-proton collisions at sqrt(s) = 13.6 TeV

CMS Collaboration

**Abstract**

We present the results about the standard muon momentum scale and resolution measurements done on the proton-proton collision data collected during the 2022, and 2023 LHC proton-proton run at 13.6 TeV. Two different techniques have been applied to respectively study medium-$p_T$ and high-$p_T$ muons, as briefly described. We found compatible the results obtained at the two different $p_T$ scales.

# Muon momentum calibration with proton-proton collisions at $\sqrt{s}$ = 13.6 TeV

The CMS Collaboration
Contacts: cms-phys-conveners-MUO@cern.ch

# Introduction

We present the corrections for bias in the measurement of the momentum of muons. Such bias can originate from a variety of sources such as detector misalignment, software reconstruction bias, and uncertainties in the magnetic field.

Corrections are derived for two different transverse momentum ($p_T$) regions, **medium $p_T$ (> 10 GeV) and high $p_T$ (> 200 GeV)** using two different approaches, both exploiting $Z \rightarrow \mu^+\mu^-$ decays produced in proton-proton collisions at 13.6 TeV and collected by the CMS experiment during 2022 and 2023.

**Data collected in 2022** are divided into two periods: **Run2022 CD (8.0 $fb^{-1}$)**, and **Run2022 EFG (26.7 $fb^{-1}$),** before and after parts of the ECAL detector were inactive due to a power cooling issue. **Data collected in 2023** are also divided into two periods: **Run2023 C (17.6 $fb^{-1}$)**, and **Run2023 D (9.5 $fb^{-1}$)**, before and after an issue observed in Barrel Pixel Layer 3, 4 (BPix3, and BPix4), in a 0.4 rad wide region around $\varphi \sim -1$ rad, which caused a loss in pixel track reconstruction.

The following **simulated events** are also used:

- **Drell-Yan + jets NLO Madgraph [1]**
- **Drell-Yan mass-binned and $p_T$-binned NLO POWHEG V2 [2-6]**

Simulated events are reconstructed with the same detector conditions of the corresponding period of data taking. The two samples are used to respectively study the medium $p_T$ and the high $p_T$ region.

[1] JHEP 07 (2014) 079 [2] JHEP 11 (2004) 040 [3] JHEP 11 (2007) 070 [4] JHEP 06 (2010) 043 [5] JHEP 07 (2008) 060 [6] JHEP 09 (2007) 126

# Medium-$p_T$ muons

# Calibration of medium $p_T$ muons

A two step method, based on the usage of $Z \rightarrow \mu^+\mu^-$ events, is used, similarly to what was done in Run2 arXiv:1208.3710

In the first step, initial correction values for the scale and resolution are obtained. The **initial scale correction,** based on the average of the $<1/p_T>$ quantity, is obtained in bins of charge (Q), η and φ. At this stage, by keeping μ+ and μ- separated, correlation among the bins are removed and an average Z boson mass value free of bias can be obtained in MC. The **initial resolution correction** is based on the difference between generated and reconstructed muon momentum in MC and obtained as a function of $p_T$ in bins of abs(η), and number of tracker layers.

In the second step the initial corrections are fine tuned to optimize the agreement between MC and data. By requiring that the reconstructed Z mass values in both data and MC are the same as for the perfectly aligned detector, **scale correction** values are respectively extracted in bins of η and φ. By requiring that the reconstructed Z peak width is the same in data and MC, **resolution corrections** for simulated muons are extracted binned abs(η).

# Event selection and simulated samples

This procedure is applied to dimuon events selected as follows:

- 2 muons with $p_T > 26$ GeV/c, with at least one matched to an isolated muon trigger object with $p_T > 24$ GeV
- both muons: $|\eta| < 2.4$ passing Tight ID [1] and Tight PFIso* [1], opposite charge
- mass selection:
  - $50 < M\mu^+\mu^- < 130$ GeV/$c^2$ for the $1/p_T$ based correction (first step)
  - $86 < M\mu^+\mu^- < 96$ GeV/$c^2$ for fine tuning (second step)

Samples:

- signal: Drell-Yan + jets NLO Madgraph [2]
- background (subtracted from data): diboson (WW, WZ, ZZ) LO pythia [3], TTBar NLO POWHEG V2 [4-7]

Further details about the procedure are described in the next slides.

(*) An exception is done for data taken during the late 2022 (EFG) period, for which Tracker-based[1] isolation is applied

[1] JINST 13 (2018) no.06, P06015 [2] JHEP 07 (2014) 079 [3] SciPost Phys. Codebases 8 (2022) [4] JHEP 11 (2004) 040 [5] JHEP 11 (2007) 070 [6] JHEP 06 (2010) 043 [7] JHEP 09 (2007) 126

# Step 1.1: extraction of the $\langle 1/p_T \rangle$ correction

**Aim:** mitigate residual bias in the muon momentum scale coming from magnetic field and alignment mismodelling

**Modelling assumptions:**

1. multiplicative correction for the magnetic field mismodelling (charge independent)
2. additive correction for alignment mismodelling (charge dependent)

**Procedure:**

Extract multiplicative parameter M and additive parameter A by solving the equation system in bins of $\eta$, $\varphi$

a. $\langle 1/p_T \rangle_{gen,\,neg} = M \langle 1/p_T \rangle_{reco,\,neg} - A$
b. $\langle 1/p_T \rangle_{gen,\,pos} = M \langle 1/p_T \rangle_{reco,\,pos} + A$

**Application:** $1/p_T \rightarrow M*1/p_T + q*A$ (raw correction fine-tuned in step 2.2)

# Step 1.2: smearing of the MC Gen-level quantities

**Aim:** smear the MC gen-level quantities so that resolution of the generator-level muon $p_T$ matches the one of the reconstructed-level muon $p_T$

**Modelling assumptions:**

1. The $p_T$ resolution primarily depends on the detector region abs(η), the number of tracker layers $n_L$, and $p_T$
2. The resolution can be described at first order by the standard deviation, remaining effects are caught by a double sided crystal ball function (dsCB)
3. The dependence of the $p_T$ resolution on $p_T$ can be modelled with a second order polynomial

**Derivation procedure** (in bins of abs(η) and $n_L$):

1. Calculate std $\sigma_R$ of the quantity $R = p_{T,\,gen} / p_{T,\,reco}$ in bins of $p_T$, abs(η) and $n_L$
2. Fit second order polynomial to $\sigma_R(p_T)$ in bins of abs(η) and $n_L$
3. Fit dsCB to the pull $(R-\langle R\rangle)/\sigma_R$ in bins of $p_T$, abs(η) and $n_L$

**Application:** In principle: $p_{T,\,gen} \rightarrow p_{T,\,gen}\,[1 + \sigma_R(p_T)\ \text{random(dsCB)}]$, but this is only needed as input for step 2.3

# Step 2.1: fine tuning (momentum scale)

**Aim:** fine tune the scale corrections obtained in step 1 by using the Z peak. Data and reco-MC momenta are scaled to match the generator dimuon mass peak position

**Modelling assumptions (in addition to those of step 1):**

The remaining correction biases are small enough to be approximated by a first order Taylor series

**Derivation procedure:**

1. The impact of a shift in the muon momentum scale on Z mass peak is approximated using a Taylor expansion
2. Correlations between the two muons are mitigated by using an iterative approach
3. The multiplicative parameter M, and the additive parameter A are iteratively updated

**Application:** $1/p_T \rightarrow M^* 1/p_T + q^*A$

# Step 2.2: fine tuning (momentum resolution)

**Aim:** fine tune the muon $p_T$ resolution in MC by extending the smearing to perfectly match data

**Modelling assumptions:**

1. Additional smearing of the muon momentum is proportional to the resolution extracted at step 2.1
2. The resolution in data is worse than the one in MC

**Derivation procedure** (in bins of abs(η)):

1. Apply additional smearing $k_{MC}$ to generated muons until the Gen dimuon mass distribution perfectly reproduces the reco-MC Z mass distribution
2. Apply additional smearing $k_{data}$ to generated muons until the Gen dimuon mass distribution perfectly reproduces the one of data

The perfect match is quantified by optimizing the $\chi^2$-value between the additionally smeared generator dimuon mass distribution, and the corresponding (unsmeared) reco-MC or data distribution

**Application:** $p_{T,\,gen} \rightarrow p_{T,\,gen}\,[1 + (k_{data} - k_{MC})^{0.5}\,\sigma_R(p_T)\,\mathrm{random(dsCB)}]$

# Muon scale and resolution corrections: Run2022 CD

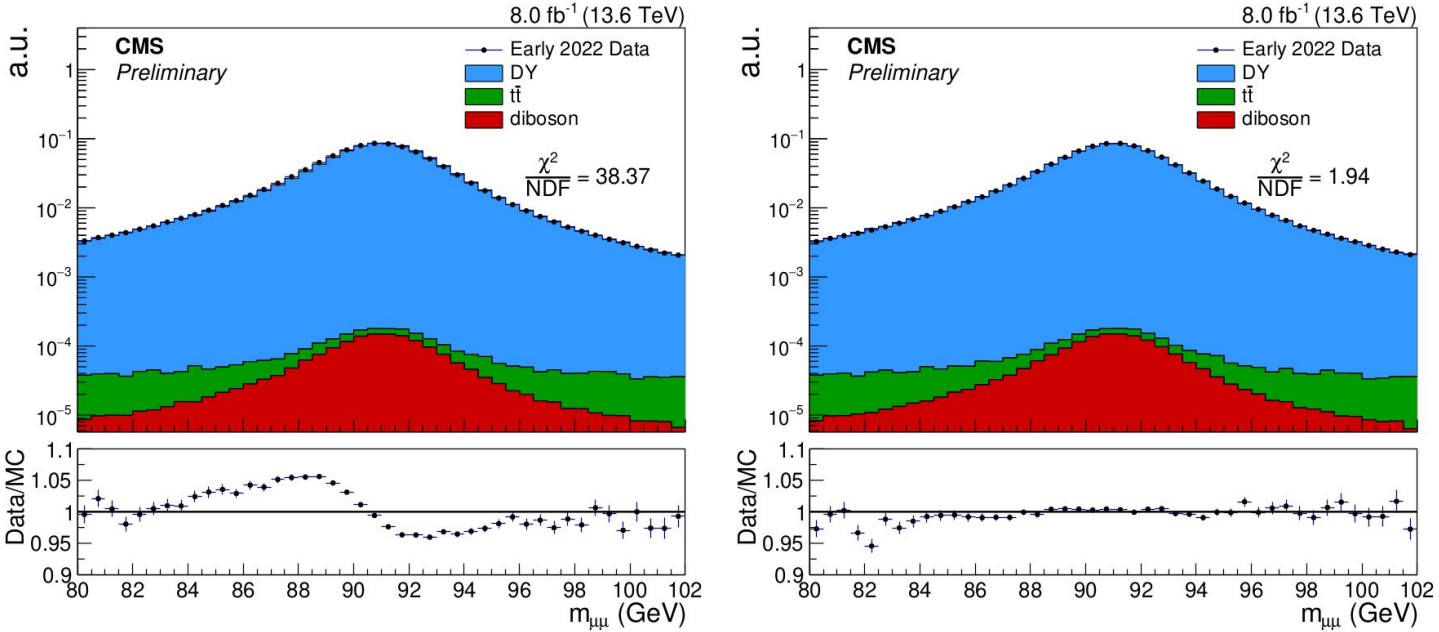


Figure 1: Effect of the muon scale and resolution corrections on the dimuon mass distribution for Run2022 CD data taking period. Uncorrected data and MC distributions are on the left, corrected distributions are on the right. The main residual background processes (1%) are shown in red and green.

# Muon scale and resolution corrections: Run2022 EFG

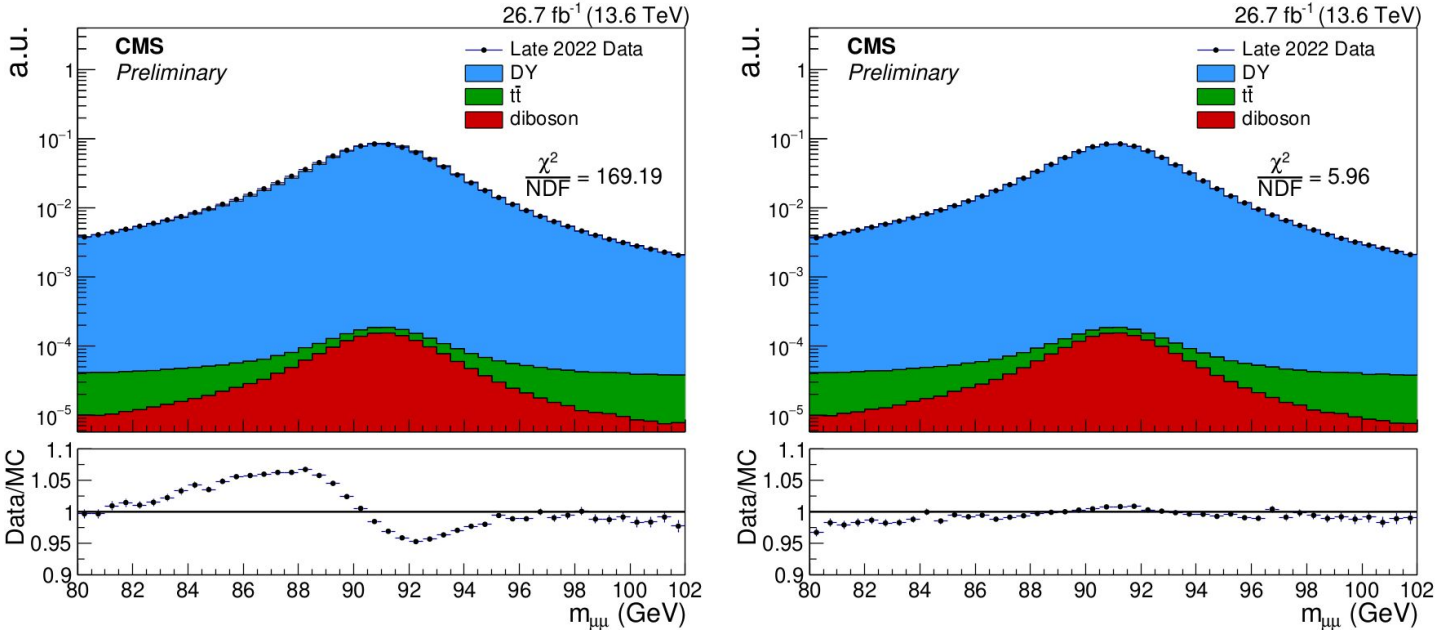


Figure 2: Effect of the muon scale and resolution corrections on the dimuon mass distribution for Run2022 EFG data taking period. Uncorrected data and MC distributions are on the left, corrected distributions are on the right. The main residual background processes (1%) are shown in red and green. Due to a different tune in the PFIso of 2022E (reprocessed) and 2022FG (not reprocessed), scale and resolution corrections are derived using events selected using the Tracker-based isolation.

# Muon scale and resolution corrections: Run2023 C

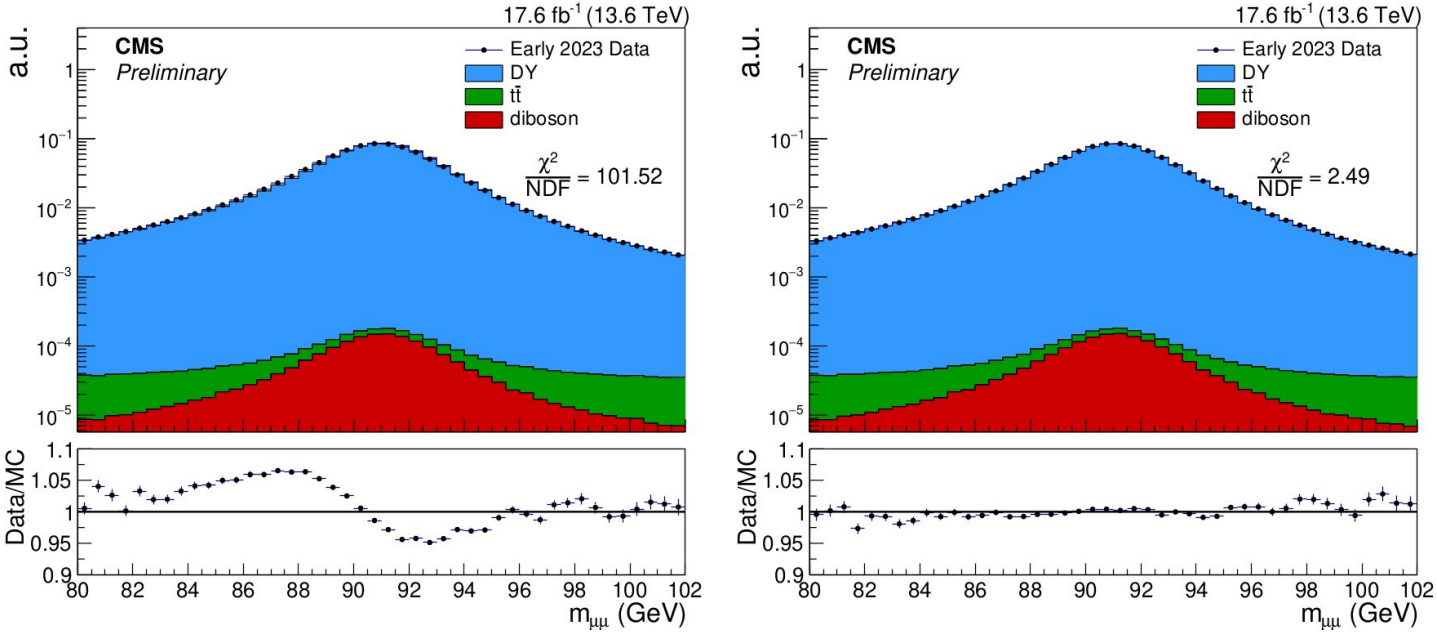


Figure 3: Effect of the muon scale and resolution corrections on the dimuon mass distribution for Run2023 C data taking period. Uncorrected data and MC distributions are on the left, corrected distributions are on the right. The main residual background processes (1%) are shown in red and green.

# Muon scale and resolution corrections: Run2023 D

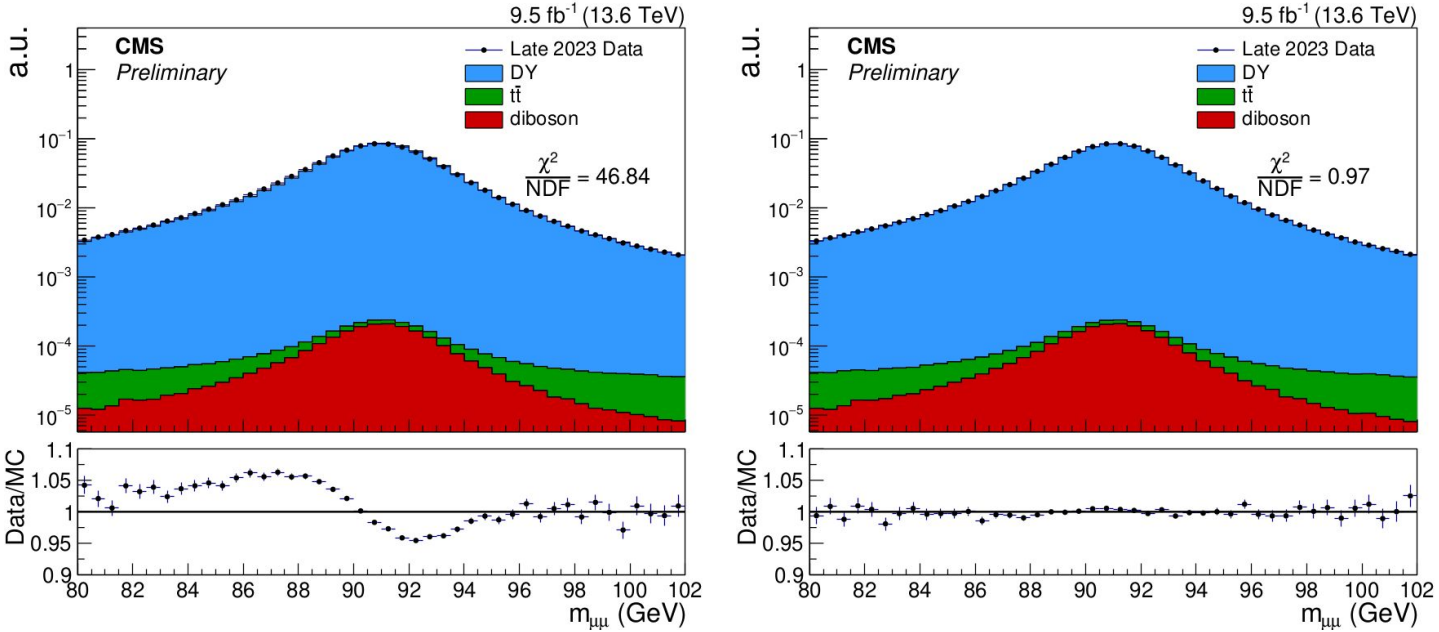


Figure 4: Effect of the muon scale and resolution corrections on the dimuon mass distribution for Run2023 D data taking period. Uncorrected data and MC distributions are on the left, corrected distributions are on the right. The main residual background processes (1%) are shown in red and green.

# High-$p_T$ muons

# Muon momentum scale bias in the high-$p_T$ regime

Bias in the muon momentum scale for **high-$p_T$ muons** is estimated using the **Generalized Endpoint method** [1]. This method consists in injecting a set of hypothetical values of bias in the simulated **muon curvature ($\kappa = q/p_T$)**, choosing as the most reliable the one that minimizes the $\chi^2$ of the difference between the curvature measured in data and the one hypothesized in MC. This bias is derived in different bins of $\eta$ and $\varphi$ for muons with a transverse momentum, $p_T$, larger than 200 (110) GeV and $|\eta| < 2.1$ ($> 2.1$).

This procedure is applied to dimuon events selected as follows:

- leading muon: TuneP $p_T > 53$ GeV/c matched to a muon trigger object with $p_T > 50$ GeV or to a tracker muon trigger object with $p_T > 100$ GeV
- subleading muon: TuneP $p_T > 25$ GeV/c
- both muons: $|\eta| < 2.4$ passing High-$p_T$ ID & TkIso < 10%
- mass selection: $M\mu^+\mu^- > 55$ GeV/$c^2$
- only to derive the bias on $\kappa$: $-5\ (-9) < \kappa < 5\ (9)$ → selecting muons $p_T > 200\ (100)$ GeV/c in barrel (endcaps)

Additional samples for background simulation:

- Di-boson (ZZ) LO Madgraph [2]
- Di-boson (WW, WZ) and TTBar NLO POWHEG V2 [3-7]
- Single Top NLO aMC@NLO V2 [2]

[1] CMS-MUO-17-001 [2] JHEP 07 (2014) 079 [3] JHEP 11 (2004) 040 [4] JHEP 11 (2007) 070 [5] JHEP 06 (2010) 043 [6] JHEP 07 (2008) 060 [7] JHEP 09 (2007) 126

# $q/p_T$ distribution in 2022

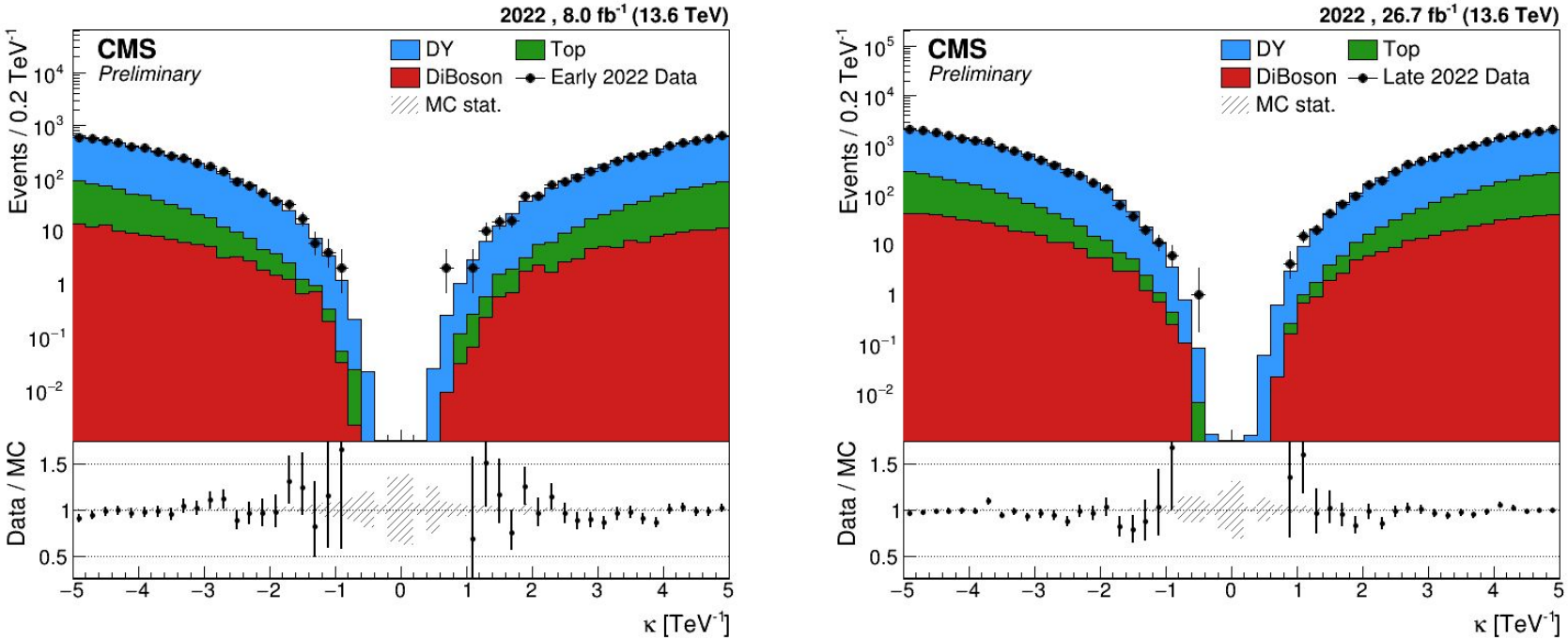


Figure 5: Data to simulation comparison of the curvature distribution, κ, in dimuon events with Run2022 CD (left) and Run2022 EFG (right) data. The muon curvature of the simulation is shown without any additive bias. Plots are inclusive in η, values of $|\kappa| < 5$ implies that muons have $p_T > 200$ GeV/c.

# $q/p_T$ distribution in 2023

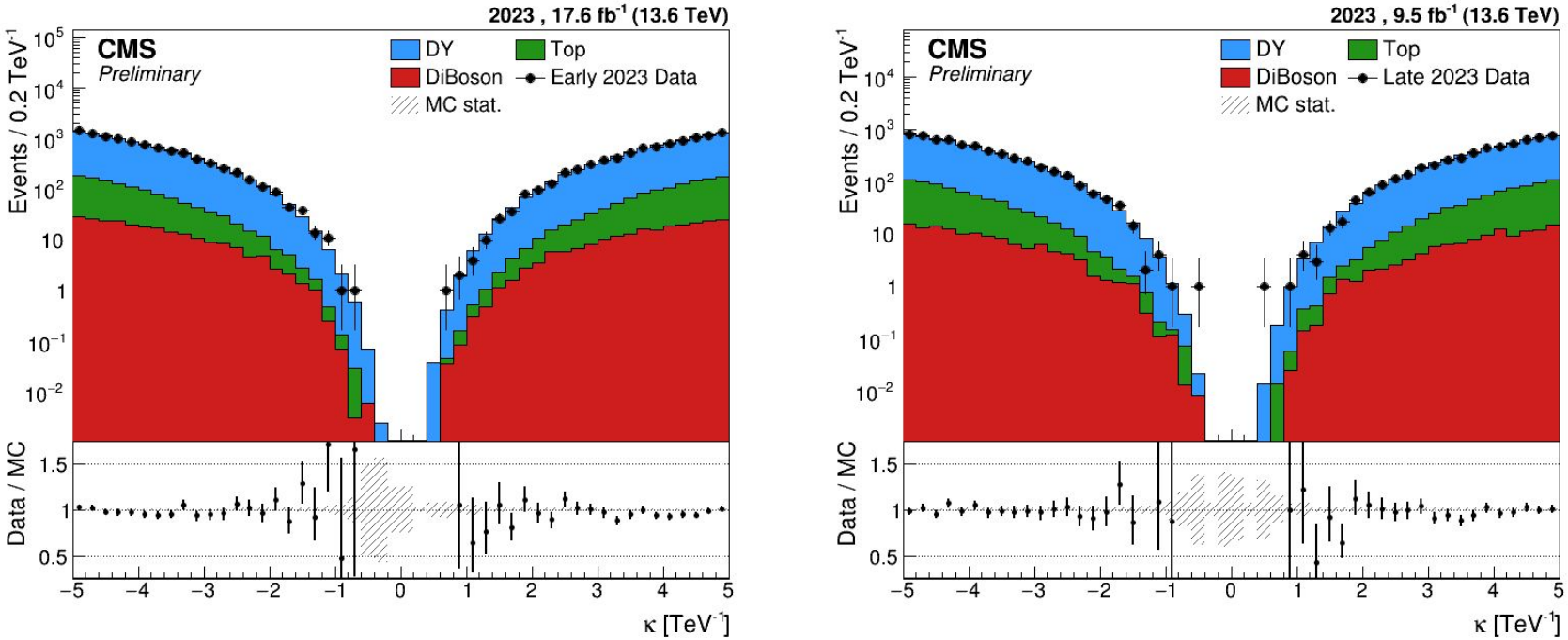


Figure 6: Data to simulation comparison of the curvature distribution, κ, in dimuon events with Run2023 C (left) and Run2023 D (right) data. The muon curvature of the simulation is shown without any additive bias. Plots are inclusive in η, values of $|\kappa| < 5$ implies that muons have $p_T > 200$ GeV/c.

# Extraction of bias on the curvature distribution

To estimate the value of bias on the curvature, $\kappa_b$, a set of values in the range [-0.8, 0.8] $TeV^{-1}$ in steps of 0.01 $TeV^{-1}$ are injected, and the $\chi^2$ distribution is derived as:

$$\chi^2(\kappa_b) = \sum_i^{nBins} \left( n^i_{data} - n^i_{MC}(\kappa_b) \right)^2$$

Results are fitted by a sum of a second order polynomial for the minimum plus and sixth order polynomial for the tails (plots for all the years are shown in backup).

For each bin of $\eta$ and $\varphi$, $\kappa_b$ value is chosen as the one minimizing the $\chi^2(\kappa_b)$ distribution, shown in Figure 7.

$\kappa_b$ distributions for 2022 and 2023 data are shown in the following slides

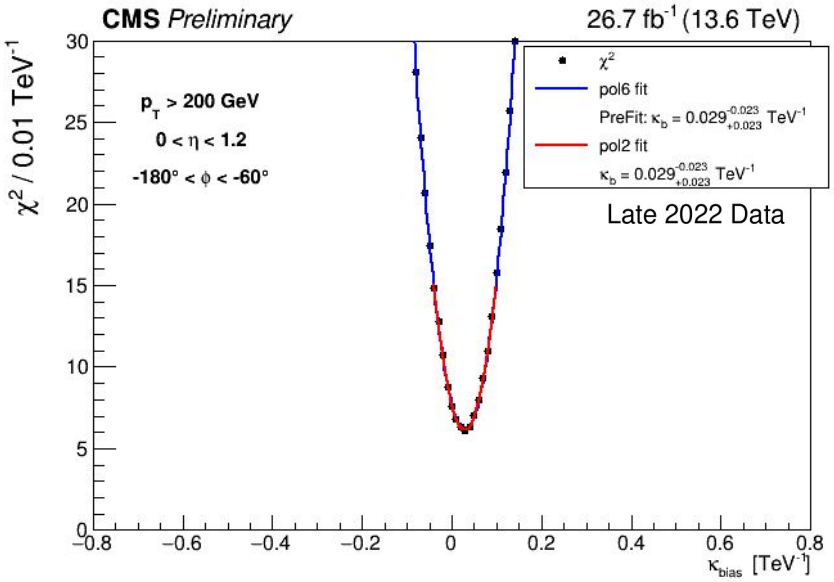


Figure 7: Example of the $\chi^2$ distribution of the data to simulation comparison as a function of the additional bias, $\kappa_b$ , added to the simulation to reproduce the scale bias present in data. $\chi^2$ test shown in this plot is done for a given bin of $\eta$ and $\varphi$, and the best value is used as input in $\kappa_b$ distributions shown in the next figures.

# Momentum scale bias for high-$p_T$ muons in 2022

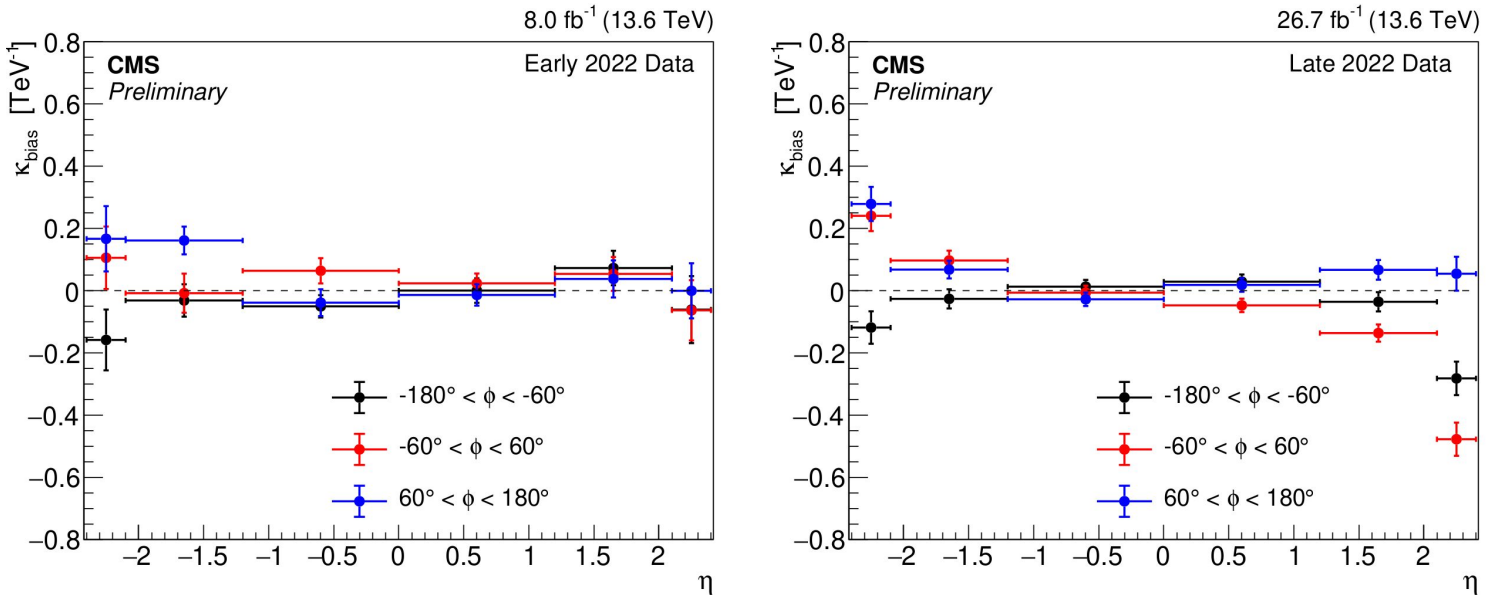


Figure 8: Measurement of the muon momentum scale bias as a function of η and φ for high-$p_T$ muons with Run2022 CD (left) and Run2022 EFG (right) data. Within the statistical uncertainty up to $|\eta| < 2.1$ no bias is observed, while a shift in the scale is measured in the very forward region of the detector. In this case, no significant differences are found when comparing TuneP $p_T$ and tracker $p_T$ , thus the bias is mostly dominated by the tracker component consistently with what measured for muons in the medium $p_T$ range. The same behaviour was also observed for the Run2 measurements.

# Momentum scale bias for high-$p_T$ muons in 2023

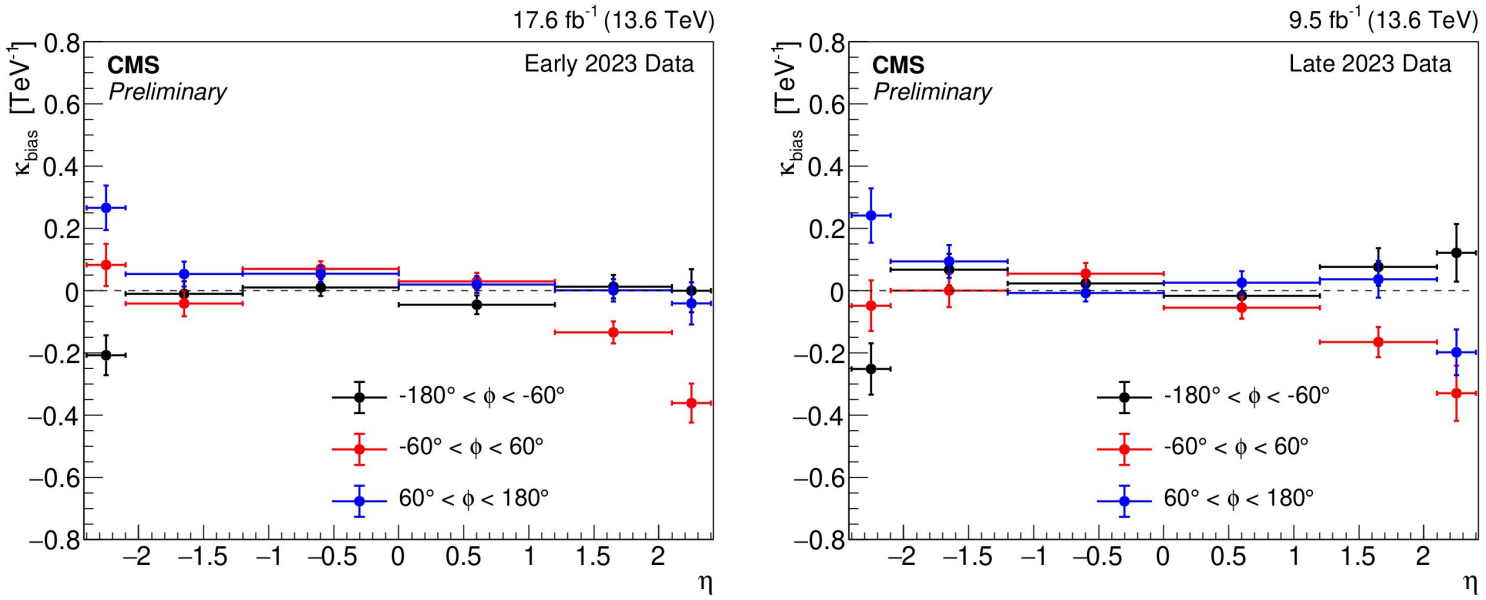


Figure 9: Measurement of the muon momentum scale bias as a function of η and φ for high-$p_T$ muons with Run2023 C (left) and Run2023 D (right) data. Within the statistical uncertainty up to $|\eta| < 2.1$ no bias is observed, while a shift in the scale is measured in the very forward region of the detector. In this case, no significant differences are found when comparing TuneP $p_T$ and tracker $p_T$ , thus the bias is mostly dominated by the tracker component consistently with what measured for muons in the medium $p_T$ range. The same behaviour was also observed for the Run2 measurements.

# Muon momentum resolution in the high-$p_T$ regime

The **muon momentum resolution** for **high-$p_T$ muons** can be measured in collision data by exploiting the dimuon mass resolution of events from the Z boson decays. The detailed procedure was developed and used in Run2 [1].

To extract the dimuon mass resolution, a dimuon mass distribution is created and fitted for different $p_T$ and $\eta$ ranges relative to the individual muon. Three different functions are convoluted with a **Breit-Wigner** to perform the dimuon mass fit: a **Crystal Ball** to extract the nominal value, a **Cruijff,** and a **Double-sided Crystal Ball** to extract the systematic variations. The same procedure is applied to both data and simulated events.

This procedure is applied to dimuon events selected as follows in both data and MC:

- muon selection: TuneP $p_T > 53$ GeV/c, $|\eta| < 2.4$, passing High-$p_T$ ID & TkIso < 10%
- $\Delta p_T/p_T < 0.3$
- at least 1 muon to a muon trigger object with $p_T > 50$ GeV or to a tracker muon trigger object with $p_T > 100$ GeV
- dimuon vertex $\chi^2 < 20$
- mass selection: $75 < M_{\mu^+\mu^-} < 105$ GeV/$c^2$

Data and MC distributions of the dimuon mass as a function of the muon $p_T$ are compared in the next slides. In almost all the cases muon momentum of simulated events is smeared to correctly describe the dimuon mass resolution obtained with data.



[1] CMS-MUO-17-001

# Muon resolution in the high-$p_T$ regime: Run2022 CD

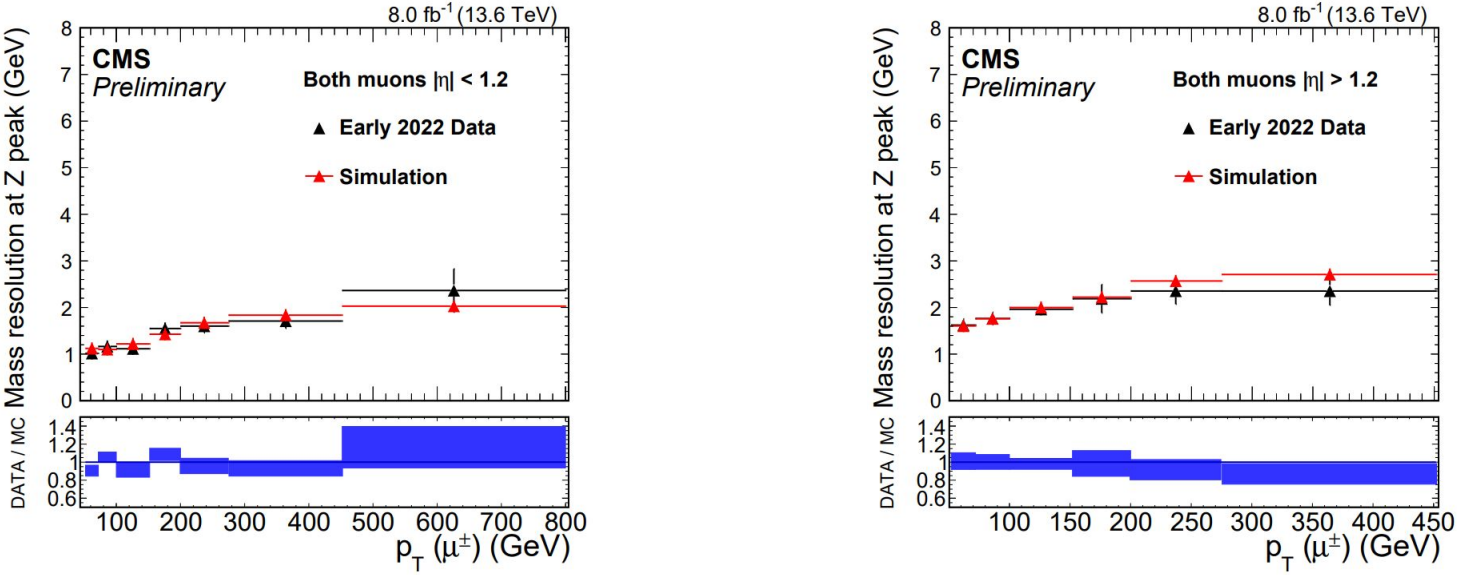


Figure 10: Measurement of the dimuon mass resolution as a function of the muon $p_T$ with Run2022 CD data. The results are further split in barrel (left, $|\eta|<1.2$) and endcap (right, $|\eta|>1.2$) regions. The $p_T$ of the simulated muons in the forward region is smeared by a 5% to correctly match the data. Only statistical error are represented in the plots, even though an additional flat 10% of systematic uncertainty has been measured by varying fit functions, fit window, and bin widths.

# Muon resolution in the high-$p_T$ regime: Run2022 EFG

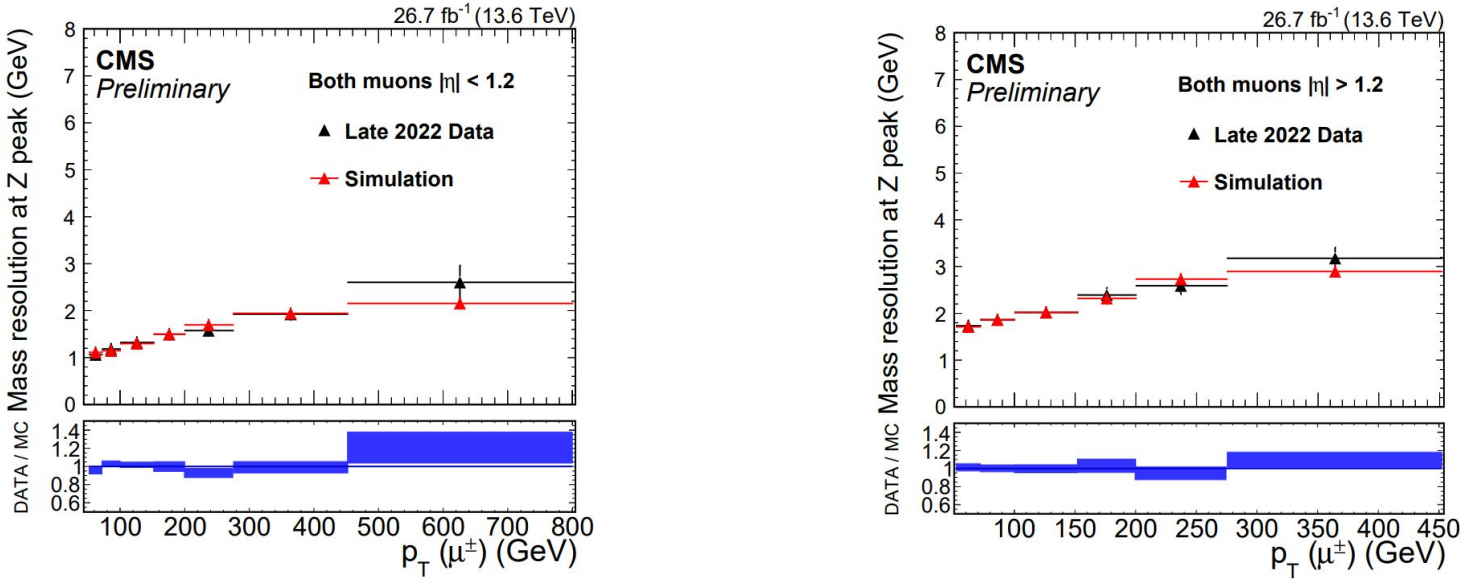


Figure 11: Measurement of the dimuon mass resolution as a function of the muon $p_T$ with Run2022 EFG data. The results are split in barrel (left, $|\eta|<1.2$) and endcap (right, $|\eta|>1.2$) regions. The $p_T$ of the simulated muons is smeared by a 5% in the barrel region and a 10% in the forward region to correctly match the resolution of data. Only statistical error are represented in the plots, even though an additional flat 10% of systematic uncertainty has been measured by varying fit functions, fit window, and bin widths.

# Muon resolution in the high-$p_T$ regime: Run2023 C

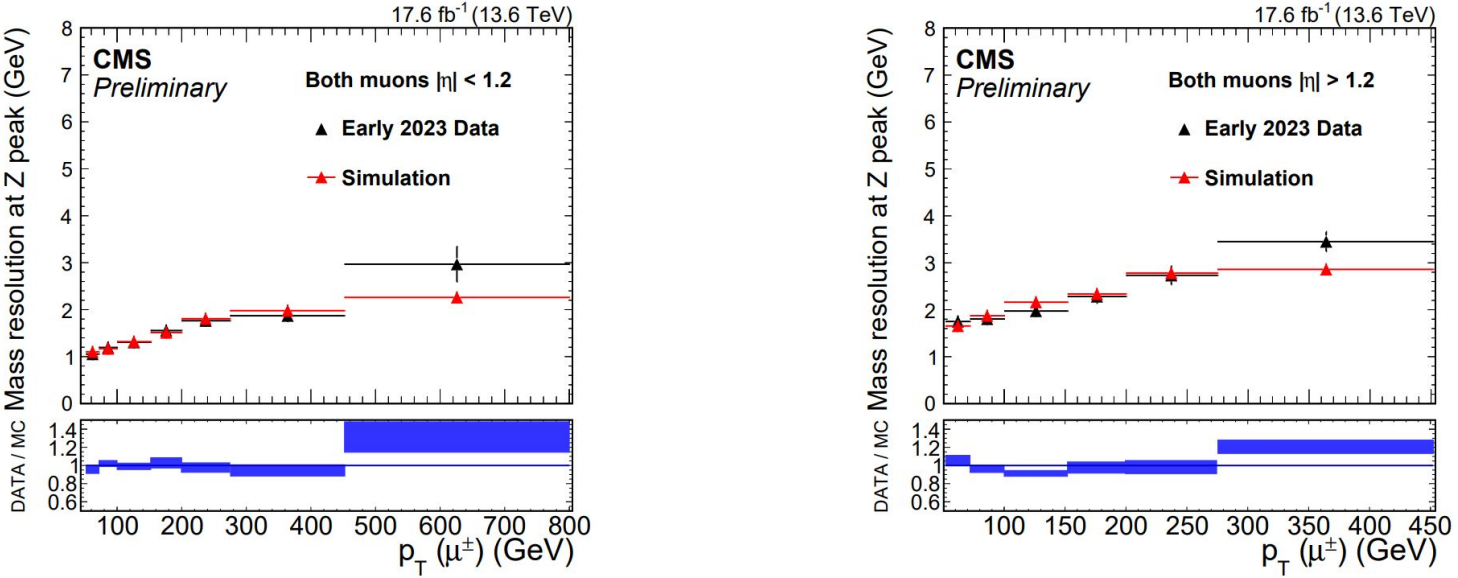


Figure 12: Measurement of the dimuon mass resolution as a function of the muon $p_T$ with Run2023 C data. The results are split in barrel (left, $|\eta|<1.2$) and endcap (right, $|\eta|>1.2$) regions. The $p_T$ of the simulated muons is smeared by a 5% in the barrel region and a 10% in the forward region to match the resolution obtained with data. Only statistical error are represented in the plots, even though an additional flat 10% of systematic uncertainty has been measured by varying fit functions, fit window, and bin widths.

# Muon resolution in the high-$p_T$ regime: Run2023 D

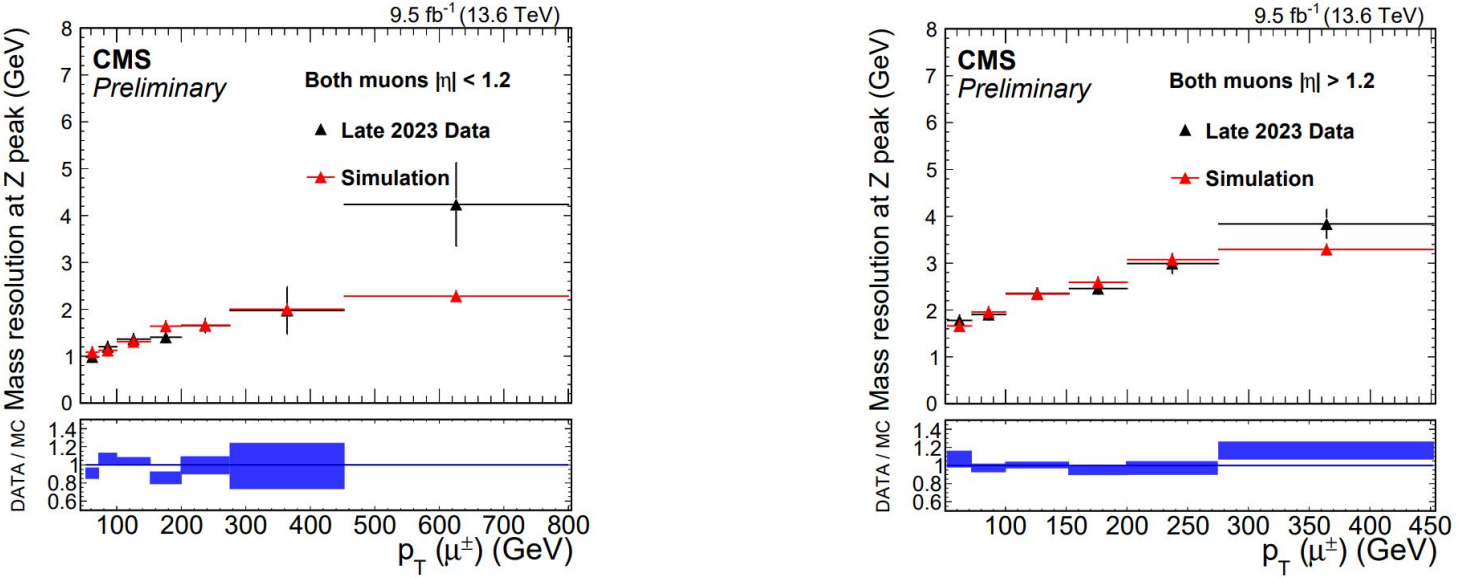


Figure 13: Measurement of the dimuon mass resolution as a function of the muon $p_T$ with Run2023 D data. The results are split in barrel (left, $|\eta|<1.2$) and endcap (right, $|\eta|>1.2$) regions. The $p_T$ of the simulated muons is smeared by a 15% in the forward region to correctly match the resolution obtained with data. Only statistical error are represented in the plots, even though an additional flat 10% of systematic uncertainty has been measured by varying fit functions, fit window, and bin widths.